



## OPEN

## SUBJECT AREAS:

CELL GROWTH  
CELL ADHESION  
CELL POLARITY  
CELLULAR IMAGINGReceived  
27 June 2013Accepted  
3 September 2013Published  
24 September 2013Correspondence and  
requests for materials  
should be addressed to  
L.J.N. (lnelson1@  
staffmail.ed.ac.uk)

# Profiling the Impact of Medium Formulation on Morphology and Functionality of Primary Hepatocytes *in vitro*

Leonard J. Nelson<sup>1</sup>, Philipp Treskes<sup>1</sup>, A. Forbes Howie<sup>2</sup>, Simon W. Walker<sup>2</sup>, Peter C. Hayes<sup>1</sup> & John N. Plevris<sup>1</sup><sup>1</sup>Hepatology Laboratory, University of Edinburgh, Chancellor's Building, Royal Infirmary of Edinburgh, EH16 4SB, Scotland, UK, <sup>2</sup>Dept of Clinical Biochemistry, University of Edinburgh, Chancellor's Building, Royal Infirmary of Edinburgh, EH16 4SB, Scotland, UK.

The characterization of fully-defined *in vitro* hepatic culture systems requires testing of functional and morphological variables to obtain the optimal trophic support, particularly for cell therapeutics including bioartificial liver systems (BALs). Using serum-free fully-defined culture medium formulations, we measured synthetic, detoxification and metabolic variables of primary porcine hepatocytes (PPHs) - integrated these datasets using a defined scoring system and correlated this hepatocyte biological activity index (HBAI) with morphological parameters. Hepatic-specific functions exceeded those of both primary human hepatocytes (PHHs) and HepaRG cells, whilst retaining biotransformation potential and *in vivo*-like ultrastructural morphology, suggesting PPHs as a potential surrogate for PHHs in various biotech applications. The HBAI permits assessment of global functional capacity allowing the rational choice of optimal trophic support for a defined operational task (including BALs, hepatocellular transplantation, and cytochrome P450 (CYP450) drug metabolism studies), mitigates risk associated with sub-optimal culture systems, and reduces time and cost of research and therapeutic applications.

There has been a resurgence of interest in the use of PPHs for biotechnology applications including cellular xeno-transplantation and BAL therapies<sup>1-3</sup>. Recent insights also support the use of PPHs as authentic surrogates for PHHs, given their similar phenotype and function<sup>4-6</sup>. Availability of PHHs for cell-based approaches to treat acute liver failure (ALF) is severely restricted due to a shortage of donor organs. As such, harnessing the potential of PPHs could herald a significant stimulus to the biotechnology sector<sup>7</sup>. In fact, BAL devices representing the most sophisticated approaches for treating ALF in a clinical setting, mostly utilize pig hepatocytes as their functional component<sup>8</sup>, whilst intracorporeal liver replacement using PPHs targeting diseased liver foci, is feasible through 3D scaffold-based tissue engineering strategies<sup>3,9-11</sup>. Critically, in all systems up to date, no transmission of porcine endogenous retroviruses was detected<sup>12</sup>.

For such diverse applications, maintenance of liver-specific functions will require appropriate microenvironmental and hepatotrophic support.

PPHs offer many advantages for BAL systems and hepatocellular transplantation (HTx) strategies for treatment of human ALF in terms of sufficient yield, viability and biocompatibility<sup>13</sup>. Indeed the pig is the most suitable non-primate species available to provide the estimated 20% (of whole liver) functional liver cell mass required for support; equivalent to approximately 20 billion hepatocytes<sup>14,15</sup>. PPHs exhibit differentiated function in culture and have a higher intrinsic metabolic activity compared to other mammalian hepatocytes<sup>16-18</sup>. Furthermore, several studies have shown that pig hepatocytes are similar to human in form, phenotype and function including biotransformation potential and hepatic phase I drug metabolism via CYP450 substrates<sup>4,5</sup>.

The primary requirement of any therapeutic application of hepatocytes is the preservation of *in vivo*-like metabolic functions. Replacement of impaired liver functions on a temporary basis may sustain life by preventing and/or decreasing the progress of hepatic encephalopathy and/or create conditions for native liver regeneration of functional tissue and full recovery<sup>19,20</sup>. Whilst the precise metabolic functions required of hepatocytes to treat ALF



are unknown, it is likely that a full repertoire of *in vivo*-like differentiated functions including synthetic, detoxifying and metabolic capabilities are prerequisites of xenogeneic hepatocytes in order to support the failing liver.

Deterioration of both liver-specific metabolic activities and hepatocyte morphology occurs within days of culture<sup>21</sup>. Since hepatocyte shape and structure are considered to be intimately related to functional activity<sup>22–24</sup>, various strategies have been adopted to address this problem, such as the use of complex biomatrices, microcarriers or synthetic hollow-fibre biomembranes to improve attachment and function of cells<sup>25</sup>. An important consideration in this regard is the optimization of the PPH culture system given that the use of xeno-based serum-supplements or biomatrices (e.g. mouse sarcoma-derived Matrigel) to retain hepatic-specific functions may be unnecessary or even detrimental to cells and therapeutic efficacy of BAL devices. Indeed, non-autologous (bovine) serum is heterogeneous in composition, promotes rapid cellular dedifferentiation and selective growth of non-parenchymal cells and may contain zoonotic endotoxins<sup>26,27</sup>.

Interestingly, it was previously shown that PPHs cultured on tissue culture plastic perform equally well compared with cells grown on a variety of exogenous attachment substrates<sup>19,28</sup> or under defined, serum-free conditions on unmodified tissue culture plastic<sup>14</sup>.

Systematic investigations of the optimal medium requirements for PPH culture in BAL devices are few, perhaps reflecting the absence of standardization and diversity of culture conditions used by different laboratories, as well as extrapolation of data from rat hepatocyte studies to evaluating PPH culture systems. Previous studies have shown that the type of medium formulation modulates morphology and function of rat and sheep hepatocyte cultures<sup>29,30</sup>, as well as porcine hepatocytes on biomatrix-coated culture dishes with or without serum<sup>1,31</sup>.

Surprisingly, given the importance, and interdependency of cellular form, phenotype and function, none of these studies addressed detailed morphological parameters in parallel, to assess culture stability.

To permit a more rigorous assessment of the effects of different media formulations on differentiated biochemical functionality and morphology, PPHs were cultured on biomatrix-free (unmodified) tissue culture plastic in four separate serum-free chemically-defined media formulations: William's E (WE) Medium<sup>32,33</sup>, Medium 199 (M199)<sup>34</sup> and Medium 1640 (M1640)<sup>35</sup> are commonly used in BAL culture systems; whereas L-15 (Leibowitz) medium maintains *in vitro* differentiated function in a variety of mammalian species<sup>1</sup> and has been used in its modified formulation (ML-15)<sup>36</sup>. Identifying the optimal medium which preserves hepatic metabolic support function and morphology would be advantageous for BAL devices. This culture system also eliminates the confounding variables introduced when using serum and/or biomatrix components.

We investigated hepatic-specific synthetic, detoxifying and metabolic capabilities of PPH to show their clinically-relevant potential to fulfil the hepatic replacement function required of BAL systems, including: (i) Albumin production as an energy-requiring biosynthetic and secretory function, (ii) Urea production from ammonium chloride as a measure of detoxifying capacity, (iii) Galactose elimination to reflect the integrity of carbohydrate metabolism, and (iv) Total cytochrome P450 (tCYP450) content as an indicator of bio-transformation potential. Gross and ultrastructural features of PPHs were assessed in parallel studies.

In order to quantify global functional capacity, a scoring system (hepatocyte biological activity index; HBAI) was devised, to simplify multiple comparisons, and as an integrated measure of overall functional capability. The biochemical data reported here were used in the generation of the HBAI, whereas parallel morphological observations were used as further validation of the comparative scores of the HBAI.

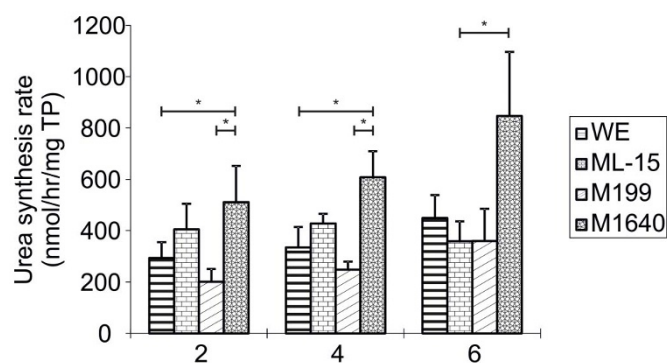


**Figure 1 | Urea Synthesis Rates in Primary Porcine Hepatocytes Cultured in Four Separate Chemically-Defined Media Formulations.** Urea synthesis rates of porcine hepatocytes cultured at  $10^7$  viable cells per 100 mm dish in WE, ML-15, M199 and M1640 chemically-defined media for up to 6 days. 2 mM  $\text{NH}_4\text{Cl}$  was added to culture dishes and incubated for 2 hours on days 2, 4 and 6. USR was determined in media samples taken at 0 and 2 hours using a modified colourimetric urea nitrogen kit as described above. Results are expressed as nmol/hour/mg total protein. All values represent the means  $\pm$  SEM of nine experiments in duplicate. Statistics: Day 2: WE vs M1640,  $p = 0.044$ ; M199 vs M1640,  $p = 0.015$ ; Day 4: WE vs M1640,  $p = 0.010$ ; M199 vs M1640,  $p = 0.001$ ; Day 6: ML-15 vs M1640,  $p = 0.031$ ; M199 vs M1640,  $p = 0.055$ .

## Results

**Cell isolation.** Cell viability of primary isolates was assessed by trypan blue exclusion test after isolation as  $87 \pm 5\%$  with a yield of  $2.2 \pm 0.8 \times 10^{10}$  viable cells from  $12 \pm 1$  kg piglets<sup>14</sup>. The non-parenchymal fraction was  $\approx 5\%$ ; as judged by the size ( $\leq 10 \mu\text{m}$  in diameter) and morphology (non-polygonal or stellate). For details on viability and plating efficiency after primary isolation, see supplementary information. If not stated otherwise, experiments were performed  $n = 10$  times.

**Urea synthesis rates.** Between-media comparisons of USR (Urea synthesis rates) were made on each day of culture ( $n = 9$ , Fig. 1). PPHs cultured in M1640 medium on day 2 of culture showed significantly higher ( $p < 0.05$ ) conversion of ammonium chloride to urea ( $511 \pm 141$  nmol/h/mg protein) compared to both WE medium and M199 ( $292 \pm 62$  nmol/h/mg protein;  $p = 0.044$  and  $201 \pm 50$  nmol/h/mg protein;  $p = 0.015$ , respectively). By day 4 of culture in M1640, the USR had further and significantly increased ( $608 \pm 102$  nmol/h/mg protein) compared to WE ( $335 \pm 79$  nmol/h/mg protein;  $p = 0.01$ ), M199 ( $248 \pm 31$  nmol/h/mg protein) whereas a moderate increase was observed relative to ML-15 ( $428 \pm 38$  nmol/h/mg protein;  $p = 0.078$ ). M1640 maintained a significantly higher USR capacity ( $847 \pm 249$  nmol/h/mg protein) over ML-15 on day 6 ( $359 \pm 77$  nmol/h/mg protein;  $p = 0.031$ ) and a greater conversion rate than hepatocytes cultured in WE ( $448 \pm 90$  nmol/h/mg protein;  $p = 0.074$ ) or M199 ( $360 \pm 125$  nmol/h/mg protein;  $p = 0.055$ ).

**Percentage galactose elimination.** For each day of culture, between-media comparisons of galactose elimination (GE) were made ( $n = 5$ , Fig. 2). Percentage GE for WE, ML-15, M199 and M1640 on culture day 2 were  $29 \pm 4$ ,  $17 \pm 2$ ,  $29 \pm 3$  and  $22 \pm 6\%$ , respectively. Galactose metabolism was significantly lower in ML-15 compared to both WE and M199 ( $p = 0.043$ ). By day 4, galactose was eliminated more slowly from M1640 ( $19 \pm 3$ ) than from WE ( $29 \pm 4$ ) or M199 ( $30 \pm 4$ ;  $p = 0.04$ ), only reaching significance in the latter culture. Day 6 cells maintained the ability to metabolise galactose as efficiently as earlier hepatocyte cultures.

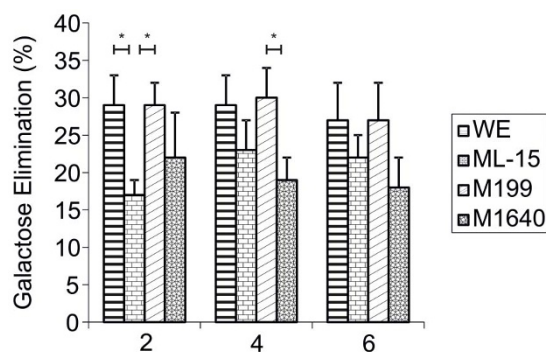


**Figure 2 | Percentage Galactose Elimination by Primary Porcine Hepatocytes Cultured in Four Separate Chemically-Defined Media Formulations.** Percentage galactose elimination of primary porcine hepatocytes cultured at  $10^7$  viable cells per 100 mm dish in WE, ML-15, M199 and M1640 chemically-defined media for up to 6 days. 1 mM D(+)-galactose was added to each culture medium and incubated for 2 hours on days 2, 4 and 6. GE was determined as above. Results are expressed as % decrease of initial [galactose]. All values represent the means  $\pm$  SEM of five experiments in duplicate. Statistics: Day 2: WE vs ML-15,  $p = 0.043$ ; ML-15 vs M199,  $p = 0.043$ . Day 4: M199 vs M1640,  $p = 0.040$ .

**Total cytochrome P450 content.** Between-media evaluations of tCYP450 (Total cytochrome P450) content were made on each day of culture ( $n = 3$ , Fig. 3). Significant differences between cells cultured in each test medium were not observed until culture days 4 and 6. tCYP450 content of ML-15 grown hepatocytes on day 4 ( $36 \pm 3$  pmol/mg protein) was significantly higher than both WE medium ( $24 \pm 3$  pmol/mg protein;  $p = 0.043$ ) or M1640 medium ( $25 \pm 5$  pmol/mg protein). tCYP450 content was significantly lower in WE medium ( $17 \pm 1$  pmol/mg protein) compared to M199 ( $28 \pm 1$  pmol/mg protein;  $p = 0.026$ ) and M1640 ( $27 \pm 5$  pmol/mg protein;  $p = 0.033$ ); and the mean value was lower, although not statistically significant, than ML-15 cultured cells ( $25 \pm 1$  pmol/mg protein;  $p = 0.071$ ).

There was a highly significant decrease in tCYP450 content, from  $120 \pm 37$  pmol/mg protein at day 0 to  $\approx 40 \pm 10$  pmol/mg protein

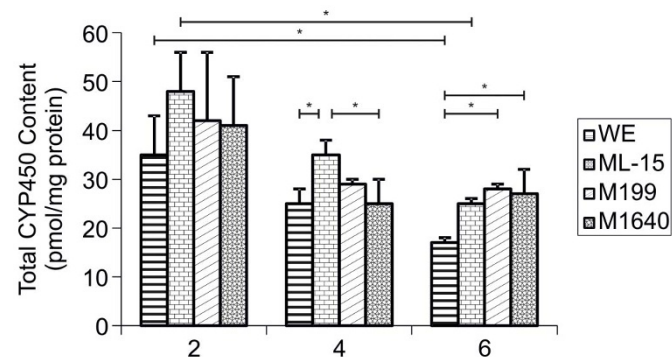


**Figure 3 | Total Cytochrome P450 Content in Primary Porcine Hepatocytes Cultured in Four Separate Chemically-Defined Media Formulations.** Total cytochrome P450 content of porcine hepatocytes cultured at  $10^7$  viable cells per 100 mm dish in WE, ML-15, M199 and M1640 chemically-defined media for up to 6 days. tCYP450 content in freshly isolated cells and cell cultures scraped from dishes on days 2, 4 and 6 was determined by carbon monoxide difference spectroscopy of the sodium hydrosulphite reduced samples as described above. Results are expressed as pmol/mg total protein. All values represent the means  $\pm$  SEM of three experiments in duplicate. Statistics: Day 4: WE vs ML-15,  $p = 0.043$ ; ML-15 vs M1640,  $p = 0.047$ . Day 6: WE vs M199,  $p = 0.026$ ; WE vs M1640,  $p = 0.033$ .

by day 2 of culture in all media formulations ( $p < 0.001$ ). tCYP450 content remained quite stable ( $\approx 30 \pm 3$  pmol/mg protein) up to day 4, but had declined significantly, when comparing day 2 values ( $\approx 40 \pm 10$  pmol/mg protein) with day 6 values in WE ( $17 \pm 1$  pmol/mg protein;  $p = 0.047$ ) and ML-15 ( $25 \pm 1$  pmol/mg protein;  $p = 0.021$ ) media formulations.

**Albumin synthesis rates.** For each medium formulation, between day comparisons were analysed ( $n = 7$ , Fig. 4). Albumin synthesis rate (ASR) by PPHs cultures remained stable up to day 4 ( $\approx 1.0$ – $1.4$   $\mu\text{g/h/mg}$  protein) but increased significantly thereafter up to day 6 of cell culture in M1640 medium ( $2.5 \pm 0.5$   $\mu\text{g/h/mg}$  protein;  $p = 0.024$ ); with substantial increases to  $2.3 \pm 0.5$   $\mu\text{g/h/mg}$  protein observed in M199 ( $p = 0.058$ ) versus  $1.7 \pm 0.4$   $\mu\text{g/h/mg}$  protein in WE medium during the same culture period. ASR could not be measured in ML-15 due to very high background levels in this proprietary medium formulation.

**Morphology of cultured hepatocytes.** The effects of medium formulation on gross cellular morphology and overall culture integrity of day 1 cultures as seen under phase contrast light microscopy are shown in Fig. 5. Plating efficiencies (see supplementary information for details) reflected the morphological observations in terms of the degree of confluency observed for each test medium and were not significantly different between media. Hepatocytes maintained in ML-15 (Fig. 5 B) and to a lesser extent, in M1640 (Fig. 5 D) display the formation of discrete colonies of piled up cells (denoted by asterisks in Fig. 5) as evidenced by the difficulty in obtaining an even plane of focus throughout the field. Monolayer formation is more evident in M1640. In contrast, cells grown in both M199 (Fig. 5 C) and WE (Fig. 5 A) media, establish more classical features of monolayer cultures although with some loosely attached cells still present.

Hepatocytes maintained for 2 days in both WE (Fig. 5 E) and M199 (Fig. 5 G) show characteristic morphology of cell culture monolayers. Hepatocyte cultures reached a completely confluent monolayer of densely packed cells, exhibiting a compact polygonal cell shape delimited by sharply-defined refractile borders containing bright nuclei under phase contrast. The lucent rim surrounding each hepatocyte represents the presence of bile canaliculi. Contrastingly, discrete cell colonies were conspicuous in ML-15- (Fig. 5 B) and

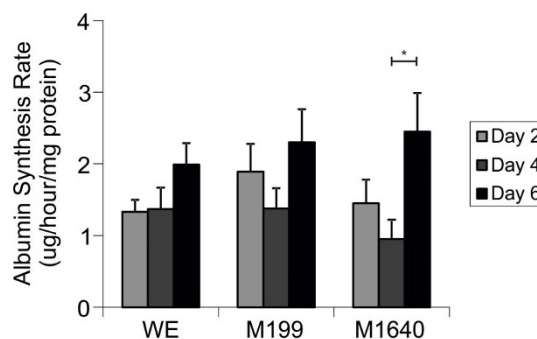


**Figure 4 | Albumin Synthesis Rates in Primary Porcine Hepatocytes Cultured in Separate Chemically-Defined Media Formulations.** Albumin synthesis rates of porcine hepatocytes seeded at  $10^7$  viable cells per 100 mm dish in WE, ML-15, M199 and M1640 chemically-defined media for up to 6 days. Samples were taken on days 2, 4 and 6 and ASR determined for each media using fluorimetric analyses of albumin blue 580 dye binding to albumin as described in *Materials and Methods*. Results are expressed as  $\mu\text{g/hour/mg}$  total protein. All values represent the means  $\pm$  SEM of 7 experiments in duplicate. Note ASR was not measured in ML-15, due to very high background levels (5% (w/v)) in this proprietary medium formulation. Statistics: M1640 d4 vs d6,  $p = 0.024$ .

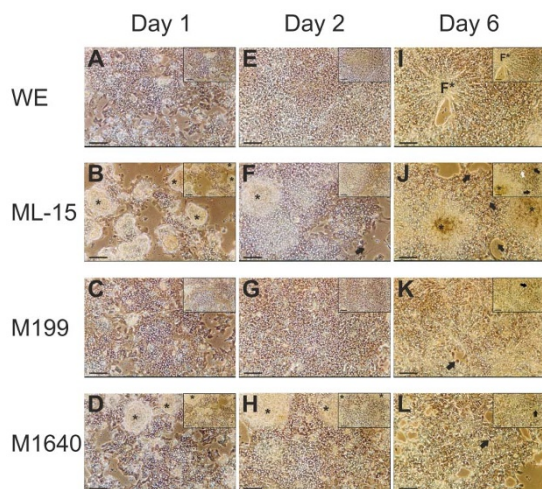


**Figure 5 | Phase contrast photomicrographs showing gross morphology of primary porcine hepatocytes cultured in four separate chemically-defined medium formulations.** Phase contrast micrographs showing gross morphology of primary porcine hepatocytes at day 1 (16 hours post-seeding), 2 and 6 in serum-free, chemically defined WE, ML-15, M199 or M1640 medium (pictures (A–L)  $\times 100$ ; scale bar  $100\ \mu\text{m}$  – inserts  $\times 200$ ; scale bar  $50\ \mu\text{m}$ ). These images show the influence of test media on the attachment efficiency or degree of confluency on culture day 1. Cells grown in both WE (A, E, I) and M199 (C, G, K) media appear as almost confluent monolayers whereas ML-15 (B, F, J) and M1640 (D, H, L) maintained cells form partial monolayers with discrete colonies of piled up cells (denoted by asterisks). As expected, the presence of non-hepatocytes in areas of low cellular density is apparent, as is the presence of bile canaliculi by highly refractive cell borders under phase contrast (C, G). After 6 days, note the appearance in WE-culture of discrete foci (denoted by F\*) of small aggregates with a radiating cord-like arrangement of hepatocytes, reminiscent of the *in vivo* cell microenvironment. However, both cell detachment and poor overall morphology compared with day 2 cultures was evident. The same was true to different degrees of degeneration for culture under the other tested media formulations as seen by cell detachment, general loss of delineating cell borders and the appearance of apoptosis, with cell blebbing (black arrows) and the appearance of lipid droplets and/or vacuoles (white arrows). Interestingly, cell colonies evident at earlier time-points under M1640 culture were no longer present.

M1640-grown (Fig. 5 H) day 2 cultures, which persisted up to day 4 in ML-15 maintained cultures (not shown). In both media, monolayers of hepatocytes were more evident than on day 1, although with areas devoid of cells. In addition, hepatocyte monolayers cultured in ML-15 and, to a lesser extent in M1640, were generally more spread out (Fig. 5 F) on the tissue culture plastic dish compared to WE and M199 cultures often showing cellular processes including pseudo-podia (Fig. 5 F, insert). These morphological characteristics were evident up to day 4 of culture (not shown).

All cultures maintained in each test medium showed distinct but varying signs of degeneration by day 6 (Fig. 5 I–L) including cell detachment, general loss or ‘blurring’ of delineating cell borders, nuclear fragmentation and the appearance of necrotic and apoptotic cells (denoted by black arrows in Fig. 5). A striking feature of WE medium was the appearance in culture of discrete foci of small cell aggregates (denoted by F\* in Fig. 5 I) with a radiating cord-like arrangement of hepatocytes reminiscent of the *in vivo* cell microenvironment. However, although cell detachment was clearly evident, hepatocyte morphology was well preserved and similar to day 4 cultures. A distinct feature of ML-15 cultures was the presence of small rounded structures, possibly lipid droplets or small vacuoles (denoted by white arrows in Fig. 5 J).

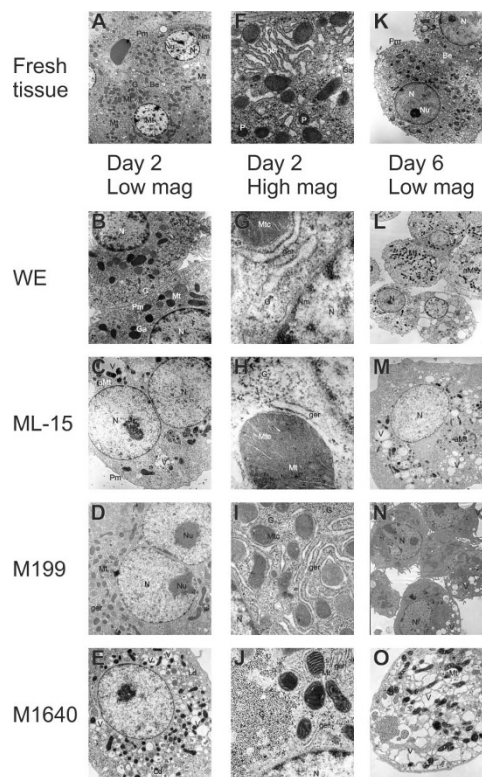


**Figure 6 | Transmission electron microscopy of fresh liver tissue and isolated hepatocytes.** Transmission electron micrographs of fresh liver tissue ((A, K)  $\times 3800$ , (F)  $\times 17000$ ) and isolated hepatocytes exhibited common fine structural features. Round nuclei (N) with nucleoli (Nu) and well-defined plasma- (Pm), nuclear (Nm) membranes and lysosomes (L), abundant mitochondria (Mt) and intact mitochondrial cristae (Mtc) and granular endoplasmic reticulum (ger) interspersed between the mitochondria. Smooth endoplasmic reticulum and golgi apparatus (Ga), peroxisomes (P) are evident, as well as numerous dense glycogen (G)  $\beta$ -particles and rosettes ( $\alpha$ -particles) between smooth endoplasmic reticulum and in close proximity to mitochondria. Bile canaliculus-like structures (Bc) are formed between adjacent hepatocytes in both fresh liver tissue and in isolated hepatocytes. Pictured hepatocytes correspond to phase contrast micrographs of day 2 and 6 displayed in Figure 5. The photomicrographs show areas of high morphological representation and were taken at the following magnifications appropriate for visualization:  $\times 3800$  (M, N),  $\times 5000$  (B, E, L),  $\times 6500$  (C, D),  $\times 10000$  (O),  $\times 28000$  (I, J) and  $\times 75000$  (G, H). Based on TEM pictures, cultures were subsequently assessed for the relative frequencies of cytoplasmic organelles and bile canaliculus-like structures on days 2 and 6 of culture for each test medium (as summarised in Table 1). Depending on the culture medium tested, a proportional reduction of intact cytoplasmic structures was observed in parallel with the occurrence of asymmetric mitochondrial swelling (aMt), the formation of lipid droplets (Ld) and extensive vacuolation (V).

Observing ultra-thin sections of cells cultured for either 2 or 6 days via transmission electron microscopy (TEM) showed that all day 2 cells had a non-polyhedral, rounded appearance probably as a result of the trypsinization process. Only WE (Fig. 6 B + G) and M199 (Fig. 6 D + I) cultured hepatocytes showed many of the classical ultrastructural features of fresh liver tissue (Fig. 6 A + F + K). In fact, some WE grown hepatocytes, uniquely, showed bile canaliculi-like structures (Fig. 6 B + G) (confirmed using fluorescein diacetate fluorescence microscopy; not shown) and Golgi saccules (with very low density lipoprotein granules). On the other hand, M199 grown hepatocytes contained a more extensive rough endoplasmic reticulum (RER) network (which correlated with a very high TP content; Fig. S1) and glycogen content (which correlated with high PAS



**Table 1 | Relative Frequencies of Cytoplasmic Organelles and Bile Canalliculi Examined Under TEM in Primary Porcine Hepatocytes on Days 2 and 6 of Culture In Chemically-Defined Serum-free Medium Formulations**

	Nuclei	Mitochondria	Ger	Glycogen Granules	Golgi Apparatus	Bile Canalliculi
<b>DAY 2</b>						
WE	+++	+++	+++	+++	+++	+++
ML-15	+++	++	+	++	+	
M199	+++	+++	+++	+++	+++	
M1640	+++	++	+	++	+	
<b>DAY 6</b>						
WE	++	++	+	++	+	+
ML-15	+	+	–	++	–	–
M199	++	++	+	++	+	–
M1640	+	+	–	–	–	–

**Table 1** shows the relative frequencies of cytoplasmic organelles and bile canalliculi-like structures in TEM sections on days 2 and 6 of culture for each test medium. Ten areas from each of 4 copper grids per sample for 3 separate isolations were investigated and the number of organelles (nuclei, mitochondria, granular endoplasmic reticulum (Ger), glycogen granules, and golgi apparatus) counted.

staining; not shown) than all other test media. In contrast, both ML-15 (Fig. 6 C + H) and M1640 (Fig. 6 E + J) cultures exhibited less mitochondria, lipid droplets, discrete fluid filled vacuoles and showed asymmetric swelling of the outer mitochondrial compartment.

By day 6, vacuolation, organellar swelling, ER vesiculation and irregular hepatocyte shape were more exaggerated and widespread in ML-15 (Fig. 6 M) and M1640 (Fig. 6 O) cultures compared with WE (Fig. 6 L) and M199 (Fig. 6 N) maintained cells.

**Relative frequencies of cytoplasmic organelles and bile canalliculi examined under TEM.** Table 1 shows a comparison of relative frequencies of cytoplasmic organelles and bile canalliculi structures on days 2 and 6 of culture for each test medium. Ten areas from each of 4 copper grids per sample for 3 separate isolations were investigated and the number of organelles (nuclei, mitochondria, granular endoplasmic reticulum (Ger), glycogen granules, and Golgi complex) counted. In addition the presence of bile canalliculi in ultra-thin sections was assessed. Day 2 cultures in WE and M199 appear to have a full complement of organelles, as observed for fresh liver sections, whereas in both ML-15- and M1640-grown hepatocytes the number of organelles is depleted. Although the relative number of organelles has declined in all media by day 6, the effects are more exaggerated in ML-15 and M1640.

**Assessment of overall performance of test media.** In order to define an index of global functional capacity, a scoring system was devised as an integrated measure of overall functional capability. Scores were generated for each test medium at each time point, by assigning an equally weighted arbitrary score of 0–10 points, for the mean values of each biochemical parameter determined from the data. Table S1 shows how comparative scores for this hepatocyte biological activity index (HBAI) were generated. The midpoint values reflect a range of values reported in the literature<sup>14,18,19,32,33,37,38</sup>. Following from this, Table 2 shows a summary of comparative scores; the rank order of test media accumulated over the 6 day culture period for each parameter and the overall ranking derived from the total score thus: M199 > WE > M1640 > ML-15.

## Discussion

Despite widespread use of culture media for cell therapeutic, pharmaceutical, and other biotechnology applications, defining the optimal medium formulation required for these modalities has not been systematically approached. The importance of identifying a culture medium which promotes hepatotrophic support, viability and differentiated function in vitro for BALs, is well recognised<sup>6,20,32,39</sup>. The aim of this study was to assess in vitro retention

of synthetic, detoxification and metabolic parameters of high-density hepatocytes cultured in fully defined WE, Modified L-15, M199 and RPMI 1640 media formulations; integrate these datasets using the HBAI to assess global functional capacity, with parallel morphological parameters to elucidate hepatotrophic support suitability.

The rationale for examining hepatocyte morphology and functional activity over a 6 day culture period follows from the fact that most porcine-based BALs are designed to be operational within 2–4 days of seeding the bioreactor using either or both a biomatrix component and serum-supplemented medium for cell support<sup>32,35,40</sup>. The majority of BALs utilise hollow fibres where porcine hepatocytes are inoculated onto various substrates which introduces unknown variables<sup>33,35,41–44</sup>. Moreover, although hepatocyte morphology is considered intimately related to function, there are few comparative studies which evaluate and correlate both parameters.

We have demonstrated that primary porcine hepatocytes can be cultured with high plating efficiency on 2D biomatrix-free tissue culture plastic in separate serum-free, chemically-defined media formulations whilst maintaining high viability and retention of significant hepatic function over six days. Assessment of overall performance of hepatocyte cultures in each test medium during this period showed that medium 199 gave the highest mean values of plating efficiency, viability, albumin synthesis rate (ASR) and percentage galactose elimination (GE). Both M199 and M1640 show differential effects on urea synthesis capacity, the latter significantly greater than all media tested (Fig. 1), and substantially higher than previously published reports<sup>6,31</sup>. Total CYP450 content remained stable in 2-day-old cultures, despite a 66% decrease compared with fresh cells although ML-15 maintained day 2 tCYP450 levels up to culture day 4. Percentage GE was relatively stable whereas ASR tended to increase in all media up to day 6. Furthermore, parallel morphological studies indicated that different medium formulations modulate gross and ultrastructural morphology of hepatocyte cultures. The results presented here are in concordance with recent assessment of comparable porcine hepatic functionality with a human HepaRG cell line-based BAL system, considered a suitable biological surrogate to PHHs<sup>45</sup>. In addition, we previously demonstrated that chemically-defined (WEM-based) trophic support promoted both 2D cultures<sup>14</sup> and 3D culture formats. Indeed the latter formed hepatospheroid structures maintained *in vivo*-like polarity, ultrastructure and differentiated functional phenotype<sup>22</sup>. Taken together these outcomes may be of relevance when choosing an appropriate medium for porcine-based BAL devices, which require rapid attachment of high viability cells with significant ammonia detoxifying capacity whilst maintaining biotransformation potential and a diverse functional profile.



Table 2 | Hepatocyte Biological Activity Index: Comparative Scores

Medium:	WE						ML-15						M199						M1640						Rank Order of Test Media			
	1	2	4	4	6	6	ST	1	2	4	4	6	6	ST	1	2	4	4	6	6	ST	1	2	4		4	6	6
USR	-	2	3	4	4	9	9	-	4	4	4	3	11	11	-	2	2	3	3	7	7	-	5	6	8	8	19	M1640>ML-15>WE>M199
GE	-	5	5	5	5	15	15	-	3	4	4	4	11	11	-	5	6	5	5	16	16	-	4	4	3	3	10	M199>WE>ML-15>M1640
ASR	-	4	4	5	13	13	13	-	-	-	-	-	-	-	-	6	4	8	18	18	-	-	-	2	8	14	M199>M1640>WE	
tCYP450	-	7	5	3	15	15	15	-	9	7	5	21	21	-	8	5	5	5	18	18	-	8	5	5	5	18	ML-15>M199=M1640>WE	
TP	7	9	9	8	33	33	33	6	7	8	9	30	30	8	10	9	9	9	36	36	7	7	8	6	28	M199>WE>ML-15>M1640		
LDH	-	10	9	9	28	28	28	-	7	9	9	25	25	-	10	10	9	9	29	29	-	8	7	6	21	M199>WE>ML-15>M1640		
Total Score	7	37	35	34	113	113	113	6	30	32	30	98	98	8	41	36	39	39	124	124	7	36	31	36	110	OVERALL RANKING (from total score): M199>WE>M1640>ML-15		

Hepatic detoxification of ammonia to urea is considered a prerequisite hepatic support function of BAL devices. Our data show highly efficient urea synthesising capacity, in agreement with previous studies<sup>19,28,32,33,37</sup> exceeding those of PPHs grown on a variety of extracellular matrices<sup>28</sup>, including Matrigel<sup>TM</sup>, considered the 'gold standard' attachment substrate promoting differentiated hepatic function. Furthermore, our values for albumin synthesis are 100× greater than those achieved using collagen gel entrapped PPHs cultured under serum-free conditions<sup>43</sup>. This reinforces the notion that (often undefined) exogenous attachment substrates, notwithstanding bio-incompatibility issues and expense, may be unnecessary for porcine-based BAL devices. Augmented urea synthesis rates may reflect: preferential cell isolation from the periportal region<sup>46</sup>; urea cycle enzyme stability; and the presence of potent stimulators of ureagenesis (arginine<sup>47</sup>, alanine, glutamine<sup>26</sup>) present in supraphysiological but variable concentrations in the test media. Indeed, arginine concentration in M1640 is 3–4 fold greater than the other media tested, and may act in synergy with released lactate<sup>26</sup> (suggested by deteriorated gross morphology, Fig. 5) to augment USR. Despite the presence of vacuoles and/or lipid deposition one can speculate that M1640-cultured hepatocytes, under stress, increase USR/ammonia removal – which is conceivably a beneficial function in the BAL setting. However, such cells would be contra-indicated for other cell therapeutic applications such as HTx, given that even with isolated cells from marginal human donor livers, low quality of such transplanted cells may be a major cause of equivocal efficacy in human clinical trials<sup>48</sup>. Indeed, ultrastructural evaluation of a porcine-based HTx strategy to treat ALF mice, showed phenotypic correlation with maintained hepatic architecture and functionality<sup>49</sup>.

Galactose elimination capacity is used as a quantitative liver function test to study functional hepatic mass<sup>50</sup> and remained stable throughout the culture period within a 20–30% range (Fig. 2) in agreement with previous reports<sup>32</sup>. Noteworthy, is that 30–35% of a galactose loading dose of 5 mmol/L is metabolized in normal individuals<sup>50</sup>. Our galactose elimination values are 2–7 fold greater (depending on the test media and culture day in our experiments) than the porcine-based BAL of Iwata *et al.*<sup>51</sup>.

A major complication of ALF is hepatic encephalopathy due in part to putative toxic compounds released from the injured liver, normally metabolised by the CYP450 system<sup>17,20,52,53</sup>. In agreement with previous observations in swine<sup>38,54</sup>, our data show that tCYP450 levels decreased but remained relatively stable over 6 days (Fig. 3). This concurred with values from serum-containing cultures of rat, mouse, hamster and human hepatocytes<sup>30,55</sup>. The labile nature of total P450 may be explained by observed down-regulation of CYP450 mRNA transcripts triggered during the collagenase isolation process<sup>56</sup>. Due to variations in the abundance and metabolic specificity of CYP450s between species, we utilised a species-independent approach by assessing 'total CYP450 content' as a measure of biotransformation potential. Total CYP450 was measured given the lack of specific antibodies/substrates for measurement of porcine CYP450. For the purpose of the HBAI more specific isoenzyme (CYP3A4 or CYP2E1) activity may be substituted for tCYP450 values in the context of PPHs or human hepatocyte cell lines, although the latter have relatively low intrinsic abundance of CYP450 activity.

Although albumin production by hepatocytes may not be a primary function required of BALs, it is a marker of hepatic-specific differentiation in culture, requiring complex processing which acts as a surrogate marker of overall cell fitness. Indeed, PPHs in all test media had double the ASR of both PPHs and HepaRG cells cultured in HepatoSTIM and WEM, respectively<sup>57</sup>.

Medium formulation appeared to have significant effects on morphological phenotype. Hepatocytes grown in WE and M199 media formulations, maintain and share most of the ultrastructural features of both fresh liver tissue and isolated hepatocytes, at least up to day 2



(Table 1). In addition hepatocytes exhibit stereotypical gross morphology – distinct nuclei and nucleoli with well-demarcated refractile cell borders up to day 4 of culture. The lucent rim surrounding each hepatocyte represents the presence of opposing membranes of bile canaliculi<sup>21,33</sup>, (Fig. 5). Distinctive attributes of the cells in these media include a full complement of organelles, as observed for fresh liver sections, and the ability of WE to preserve bile canaliculi-like structures whereas M199 appears to enhance both the glycogen and RER protein synthetic machinery (the latter correlating with a significantly higher total protein content ( $p < 0.05$ ) than both ML-15 and M1640 media; Fig. S1). This demonstrates that the type of medium influenced cell proliferation by culture day 2 with M199 in particular, apparently stimulating growth. WE and M199 show their hepatocyte nuclei to be in close proximity to enriched mitochondria, lysosomes and adjacent glycogen particles. In contrast both ML-15 and M1640 exhibited atypical gross morphology including formation of discrete colonies, and fine structural features of stressed cells including vacuolation and/or lipid deposition as well as depleted organelles (Fig. 6; Table 1). These observations suggest that preservation of such morphological markers of differentiation reflects a potential for expression of normal *in vitro* functionality. Indeed, selecting a given medium for a specific *in vitro* functional assay could be based on both HBAI as well as gross and ultrastructural properties. For example both WE and M199 show high HBAI scores coupled with demonstrable *in vivo*-like ultrastructure (Fig. 6), suggesting they may be suitable for both HTx strategies or CYP450 drug studies given CYP450s are primarily located in the ER and mitochondrial inner membranes of hepatocytes.

Despite the high viabilities evident in all test media on day 6 (Figures S1, S2), and the significant influence of ML-15 (day 2) on retained LDH activity, the morphological observations, coupled with HBAI scoring, strongly favour WE and M199 media over and above the other media used.

Defining the overall performance of media formulations is crucial for effective cell-based therapies<sup>58</sup>; whilst testing efficacy of the various BAL devices under development require a large animal model of acetaminophen-induced ALF<sup>59</sup>. However, the absence of standardization for assessment of cell function between laboratories, represents a major drawback, due to the variable usage of, for example, serum-free or serum-containing media formulations, biomatrices or culture system modalities. Such diversity of approach and our limited information of the most important hepatocyte functions make direct comparisons between research groups very difficult. It may therefore be useful to assess and weight all cell functions equally. Therefore, to simplify comparisons, we propose a HBAI, which normalises each hepatic functional parameter with respect to an equally weighted scoring system (Supplementary Table S1). Additionally, the impact of media formulation on culture morphology, including ultrastructure (Table 1; Fig. 6), and gross cell morphology (Fig. 5) are taken into account. Using these criteria it is evident that M199 attained the highest HBAI score overall (Table 2), ranking the media as follows: M199 > WE > M1640 > ML-15. This utility may allow direct comparisons of any hepatocyte-based culture system.

## Methods

**Hepatocyte isolation and culture.** All animals received humane care in compliance with the the UK Home Office Guidelines under the Animal (Scientific Procedures) Act 1986 and study protocols complied with University of Edinburgh guidelines. Hepatocytes were isolated from weanling piglets (<15 kg) using our *ex vivo* collagenase perfusion method, previously described in detail<sup>14</sup>. They were seeded at a density of  $10^7$  viable cells per 100 ml tissue culture plastic dish (Dow Corning, MI, USA) in 8 ml of Medium. The culture dishes were shaken gently for some minutes to aid dispersal of cells for attachment and placed in a humidified incubator under a 95% air: 5% CO<sub>2</sub> atmosphere at 37°C. Cells were kept in culture for 6 days and analyses were performed on days 1, 2, 4 and 6 as detailed in the following paragraphs. Medium was changed on day 1, 2 and 4.

The cells were tested against four different types of culture media. Each culture medium consisted of a serum-free, chemically-defined base medium (either Williams E (WE), (Leibowitz) modified L-15 Medium (ML-15), Medium 199 (M199), RPMI

1640 (M1640)) supplemented with 50 ng/ml Long-Epidermal Growth Factor (L-EGF); 10 µg/ml porcine insulin; 1 µmol/L dexamethasone; 2 mmol/L L-Glutamine; 50 mg/ml Gentomycin; 50 mg/ml Penicillin-Streptomycin and 2.5 µg/ml Fungizone.

**Biochemical and metabolic assessment.** For each tested medium, hepatocytes were cultured on duplicate tissue culture plastic dishes and evaluated for markers of differentiated biochemical function. On the day of isolation (day 0) and on culture days 2, 4 and 6, tCYP450 was measured. Furthermore, albumin production, GE, and USR were analysed on day 2, 4 and 6 of culture. Samples were taken from 10 separate isolations.

Total CYP450 was determined in fresh cell suspensions and after 1, 2, 4 and 6 days of test media culture in duplicate dishes to assess cellular biotransformation potential as previously described<sup>14</sup>. Briefly, fresh or cultured hepatocyte samples were solubilised in ice-cold P450 buffer, sonicated and stored at -80°C until analysis. tCYP450 content was determined by carbon monoxide difference spectroscopy of the sodium hydrosulphite-reduced samples, using a dual-beam spectrophotometer (Kontron, Switzerland). Results are expressed as pmol/mg protein.

Urea concentrations for each test medium and USR were assessed as previously described<sup>14</sup>. Briefly, on days 2, 4 and 6, duplicate cell culture dishes were washed twice with HBSS at 37°C and incubated in 8 ml of each test medium with either 2 mmol/L NH<sub>4</sub>Cl or 1 mmol/L D(+)-galactose for 2 hours<sup>32</sup> at 37°C. For reference, media controls were treated under otherwise identical conditions except without cells.

For the calculation of USR 0.5 ml samples were taken at day 2, 4 and 6 at  $t = 0$  and  $t = +2$  hours using a modified colourimetric urea nitrogen kit (Sigma, Mo, USA) according to the manufacturer's instructions. The USR was corrected for total protein content and for pre- and post-incubation volumes for each culture dish and is expressed as nmol/hour/mg TP.

Galactose concentration was determined in 0.5 ml samples taken at day 2, 4 and 6 at  $t = 0$  and  $t = +2$  hours using a modified galactose kit (Roche, UK) according to the manufacturer's instructions. Percentage GE was calculated as the amount of galactose eliminated after 2 hours expressed as a percentage of the initial value at 0 hours.

The ASR was determined based on albumin concentration in duplicate samples of culture supernatants taken on days 2, 4 and 6 using a fluorimetric albumin blue 580 dye-binding assay<sup>60</sup> optimised for measurement in cell culture supernatants. Our adaptation sought to exploit the use of a fluorescence reader for microtitre plates so that multiple samples could be analysed simultaneously.

1 ml samples were taken from duplicate cell culture dishes on days 2, 4 and 6. Pig albumin (Sigma) dissolved in calibrator diluent was used as the albumin standard and was prepared fresh for each assay run. Calibrator diluent was prepared by dissolving 2.7 g KH<sub>2</sub>PO<sub>4</sub>, 0.9 g K<sub>2</sub>HPO<sub>4</sub>, 4.5 g of sodium chloride, 0.5 g of EDTA disodium salt and 50 mg of pig gamma immunoglobulins (IgG; Sigma) in 500 ml of dH<sub>2</sub>O (pH 6.0) and stored at 4°C. Pig IgG was included as a stabilizer to prevent non-specific absorption of albumin to plastic surfaces.

**Morphological and ultrastructural assessment.** To examine gross morphology, cultured cells were examined under phase-contrast using a Telaval 20 inverted microscope (Zeiss, Germany) on days 1, 2, 4 and 6 of culture for each test medium and images captured.

To examine ultrastructural features via TEM, cells were processed as previously described<sup>22</sup>. Cells cultured in each test medium, obtained from the same isolation as used for the phase-contrast study were taken on days 2 and 6 washed in HBSS buffer to remove dead or loosely attached cells and trypsinized with [0.5×] normal trypsin-EDTA (Sigma).

Following low-speed centrifugation (20 g; 5 minutes) and washing steps in HBSS/5% FBS to neutralize trypsin activity, the cell pellet was resuspended and fixed with 3% glutaraldehyde in 0.1 M sodium cacodylate buffer solution at pH 7.3 for 2.5 hours at room temperature. Fresh liver tissue and freshly isolated cells were similarly treated as controls.

After several washings with cacodylate buffer solution the samples were post-fixed with 1% osmium tetroxide in 0.1 M cacodylate buffer solution at pH 7.3 for one hour at room temperature. Following dehydration in a graded series of acetone solutions (50, 70, 90, and 100% (3 times)), the tissue was infiltrated and embedded in araldite mixture. In order to orientate and select an area for the ultrastructural observations, semi-thin sections (1 µm in thickness) were cut with glass knives, stained with 1% toluidine blue and examined under the light microscope. Ultra-thin sections with silver gold interference colour (approximately 70–80 nm in thickness) were cut on an ultramicrotome (Ultracut OmU4, Reichert Co., Austria) and collected on 200 mesh uncoated copper grids. The sections were double stained in saturated uranyl acetate in 50% methanol for 30 minutes followed by lead citrate in water for 5 minutes. Ten areas from each of 4 copper grids were selected for investigation and representative grids examined and photographed in a scanning transmission electron microscope (CM12, Philips, UK) at 80 kV.

**Statistical analysis.** One-Way Analysis of Variance (ANOVA) was performed on 1) between-media evaluations on each day of culture, and 2) between-day evaluations for each single medium formulation followed by a *post-hoc* multiple comparisons tests of *least significant differences*, using the SPSS 9.0 statistical software package. The mean difference was considered significant at the 0.05 level. Results are expressed as mean ± SEM (standard error mean) and the number of experiments performed (n) is indicated. Statistical data is presented where relevant (significant) p-values for multiple comparisons of either or both 1) and 2) above were calculated.



1. Jasmund, I. *et al.* The influence of medium composition and matrix on long-term cultivation of primary porcine and human hepatocytes. *Biomol. Eng.* **24**, 59–69 (2007).
2. Carpentier, B., Gautier, A. & Legallais, C. Artificial and bioartificial liver devices: present and future. *Gut* **58**, 1690–1702 (2009).
3. Eksler, B. *et al.* Clinical xenotransplantation: the next medical revolution? *Lancet* **379**, 672–683 (2012).
4. Laine, J. E., Auriola, S., Pasanen, M. & Juvonen, R. O. Acetaminophen bioactivation by human cytochrome P450 enzymes and animal microsomes. *Xenobiotica*. (2009).
5. Puccinelli, E., Gervasi, P. G. & Longo, V. Xenobiotic metabolizing cytochrome P450 in pig, a promising animal model. *Curr. Drug. Metab.* **12**, 507–525 (2011).
6. Maringka, M., Giri, S., Nieber, K., Acikgöz, A. & Bader, A. Biotransformation of diazepam in a clinically relevant flat membrane bioreactor model using primary porcine hepatocytes. *Fundam. Clin. Pharmacol.* **25**, 343–353 (2011).
7. Frankish, H. Pig organ transplantation brought one step closer. *Lancet* **359**, 137 (2002).
8. Pless, G. in *Hepatocytes*. 511–523 (Humana Press, 2010).
9. Poyck, P. P. C. *et al.* In vitro comparison of two bioartificial liver support systems: MELS CellModule and AMC-BAL. *Int. J. Artif. Organs*. **30**, 183–191 (2007).
10. Fiegel, H. C. *et al.* Hepatic tissue engineering: from transplantation to customized cell-based liver directed therapies from the laboratory. *J. Cell. Mol. Med.* **12**, 56–66 (2008).
11. Lang, R. *et al.* Three-dimensional culture of hepatocytes on porcine liver tissue-derived extracellular matrix. *Biomaterials* **32**, 7042–7052 (2011).
12. Denner, J. & Tonjes, R. R. Infection barriers to successful xenotransplantation focusing on porcine endogenous retroviruses. *Clin. Microbiol. Rev.* **25**, 318–343 (2012).
13. Tsiaouassis, J., Newsome, P. N., Nelson, L. J., Hayes, P. C. & Plevris, J. N. Which hepatocyte will it be? Hepatocyte choice for bioartificial liver support systems. *Liver Transpl.* **7**, 2–10 (2001).
14. Nelson, L. J. *et al.* An improved ex vivo method of primary porcine hepatocyte isolation for use in bioartificial liver systems. *Eur. J. Gastroenterol. Hepatol.* **12**, 923–930 (2000).
15. Newsome, P. N., Plevris, J. N., Nelson, L. J. & Hayes, P. C. Animal models of fulminant hepatic failure: a critical evaluation. *Liver Transpl.* **6**, 21–31 (2000).
16. Skaanild, M. T. Porcine cytochrome P450 and metabolism. *Curr. Pharm. Des.* **12**, 1421–1427 (2006).
17. Desille, M. *et al.* Detoxifying activity in pig livers and hepatocytes intended for xenotherapy. *Transplantation* **68**, 1437–1443 (1999).
18. Donato, M. T., Castell, J. V. & Gómez-Lechón, M. J. Characterization of drug metabolizing activities in pig hepatocytes for use in bioartificial liver devices: comparison with other hepatic cellular models. *J. Hepatol.* **31**, 542–549 (1999).
19. Gregory, P. G., Connolly, C. K., Toner, M. & Sullivan, S. J. In vitro characterization of porcine hepatocyte function. *Cell Transplant* **9**, 1–10 (2000).
20. Naik, S., Trenkler, D., Santangini, H., Pan, J. & Jauregui, H. O. Isolation and culture of porcine hepatocytes for artificial liver support. *Cell Transplant.* **5**, 107–115 (1996).
21. LeCluyse, E. L., Bullock, P. L. & Parkinson, A. Strategies for restoration and maintenance of normal hepatic structure and function in long-term cultures of rat hepatocytes. *Adv. Drug. Deliv. Rev.* **22**, 133–186 (1996).
22. Nelson, L. J., Walker, S. W., Hayes, P. C. & Plevris, J. N. Low-shear modelled microgravity environment maintains morphology and differentiated functionality of primary porcine hepatocyte cultures. *Cells Tissues Organs* **192**, 125–140 (2010).
23. Barrila, J. *et al.* Organotypic 3D cell culture models: using the rotating wall vessel to study host-pathogen interactions. *Nat. Rev. Microbiol.* **8**, 791–801 (2010).
24. Mitaka, T. The current status of primary hepatocyte culture. *Int. J. Exp. Pathol.* **79**, 393–409 (2002).
25. Demetriou, A. & Rozga, J. in *Liver Growth and Repair*. 627–652 (Springer, Netherlands, 1998).
26. Berry, M., Grivell, A., Grivell, M. & Phillips, J. Isolated hepatocytes-past, present and future. *Cell. Biol. Toxicol.* **13**, 223–233 (1997).
27. Enat, R. *et al.* Hepatocyte proliferation in vitro: its dependence on the use of serum-free hormonally defined medium and substrata of extracellular matrix. *Proc. Natl. Acad. Sci. U.S.A.* **81**, 1411–1415 (1984).
28. te Velde, A. A., Ladiges, N. C. J. J., Flendrig, L. M. & Chamuleau, R. A. F. M. Functional activity of isolated pig hepatocytes attached to different extracellular matrix substrates. Implication for application of pig hepatocytes in a bioartificial liver. *J. Hepatol.* **23**, 184–192 (1995).
29. LeCluyse, E., Bullock, P., Madan, A., Carroll, K. & Parkinson, A. Influence of Extracellular Matrix Overlay and Medium Formulation on the Induction of Cytochrome P-450 2B Enzymes in Primary Cultures of Rat Hepatocytes. *Drug. Metab. Dispos.* **27**, 909–915 (1999).
30. Watts, P. *et al.* The influence of medium composition on the maintenance of cytochrome P-450, glutathione content and urea synthesis: a comparison of rat and sheep primary hepatocyte cultures. *J. Hepatol.* **23**, 605–612 (1995).
31. Schneider, C., Aurich, H., Wenkel, R. & Christ, B. Propagation and functional characterization of serum-free cultured porcine hepatocytes for downstream applications. *Cell Tissue Res.* **323**, 433–442 (2006).
32. Flendrig, L. M. *et al.* In vitro evaluation of a novel bioreactor based on an integral oxygenator and a spirally wound nonwoven polyester matrix for hepatocyte culture as small aggregates. *J. Hepatol.* **26**, 1379–1392 (1997).
33. De Bartolo, L., Jarosch-Von Schweder, G., Haverich, A. & Bader, A. A novel full-scale flat membrane bioreactor utilizing porcine hepatocytes: cell viability and tissue-specific functions. *Biotechnol. Progr.* **16**, 102–108 (2000).
34. Gerlach, J., Klöppel, K., Stoll, P., Vienken, J. & Müller, C. Gas supply across membranes in bioreactors for hepatocyte culture. *Int. J. Artif. Organs.* **14**, 328–333 (1990).
35. Kong, L. B., Chen, S., Demetriou, A. A. & Rozga, J. Matrix-induced liver cell aggregates (MILCA) for bioartificial liver use. *Int. J. Artif. Organs.* **19**, 72–78 (1996).
36. Hamilton, G., Fox, R., Atterwill, C. & Gedorge, E. Liver spheroids as a long term model for liver toxicity in vitro. *Hum. Exp. Toxicol.* **15**, 153 (1995).
37. Lazar, A. *et al.* Formation of porcine hepatocyte spheroids for use in a bioartificial liver. *Cell Transplant.* **4**, 259–268 (1995).
38. Olsen, A. K., Hansen, K. T. & Friis, C. Pig hepatocytes as an in vitro model to study the regulation of human CYP3A4: prediction of drug-drug interactions with 17 alpha-ethynylestradiol. *Chem. Biol. Interact.* **107**, 93–108 (1997).
39. Dong, J. *et al.* Evaluation and optimization of hepatocyte culture media factors by design of experiments (DoE) methodology. *Cytotechnology* **57**, 251–261 (2008).
40. Wang, L. *et al.* Comparison of porcine hepatocytes with human hepatoma (C3A) cells for use in a bioartificial liver support system. *Cell Transplant.* **7**, 459–468 (1998).
41. Maringka, M., Giri, S. & Bader, A. Preclinical characterization of primary porcine hepatocytes in a clinically relevant flat membrane bioreactor. *Biomaterials* **31**, 156–172 (2010).
42. Nyberg, S. L. *et al.* Extracorporeal application of a gel-entrapment, bioartificial liver: demonstration of drug metabolism and other biochemical functions. *Cell Transplant.* **2**, 441–452 (1993).
43. Sielaff, T. D. *et al.* A technique for porcine hepatocyte harvest and description of differentiated metabolic functions in static culture. *Transplantation* **59**, 1459–1463 (1995).
44. Yu, Y. *et al.* Cell therapies for liver diseases. *Liver Transpl.* **18**, 9–21 (2012).
45. Nibourg, G. A. *et al.* Liver progenitor cell line HepaRG differentiated in a bioartificial liver effectively supplies liver support to rats with acute liver failure. *PLoS One* **7**, e38778 (2012).
46. Kano, J., Tokiwa, T., Zhou, X. & Kodama, M. Colonial growth and differentiation of epithelial cells derived from abattoir adult porcine livers. *J. Gastroenterol. Hepatol.* **13** Suppl, S62–69 (1998).
47. Ampola, M. in *The Liver, Biology and Pathobiology*. 365–377 (Raven Press, New York, 1994).
48. Fox, I. J. & Roy-Chowdhury, J. Hepatocyte transplantation. *J. Hepatol.* **40**, 878–886 (2004).
49. Yamamoto, T. *et al.* Treatment of acute liver failure in mice by hepatocyte xenotransplantation. *Cell Transplant.* **19**, 799–806 (2010).
50. Kaplowitz, N. *Liver and biliary diseases*. (Williams & Wilkins, 1992).
51. Iwata, H. *et al.* In vitro evaluation of metabolic functions of a bioartificial liver. *ASAIO J.* **45**, 299–306 (1999).
52. Blei, A. T. Medical therapy of brain edema in fulminant hepatic failure. *Hepatology* **32**, 666–669 (2000).
53. Jauregui, H. O. & Gann, K. L. Mammalian hepatocytes as a foundation for treatment in human liver failure. *J. Cell. Biochem.* **45**, 359–365 (1991).
54. Monshouwer, M., van't Klooster, G. A. E., Nijmeijer, S. M., Witkamp, R. F. & van Miert, A. S. J. P. A. M. Characterization of cytochrome P450 isoenzymes in primary cultures of pig hepatocytes. *Toxicol. In Vitro* **12**, 715–723 (1998).
55. Chesne, C. *et al.* Viability and function in primary culture of adult hepatocytes from various animal species and human beings after cryopreservation. *Hepatology* **18**, 406–414 (1993).
56. Padgham, C. R. & Paine, A. J. Altered expression of cytochrome P-450 mRNAs, and potentially of other transcripts encoding key hepatic functions, are triggered during the isolation of rat hepatocytes. *Biochem. J.* **289** (Pt 3), 621–624 (1993).
57. Lubberstedt, M. *et al.* HepaRG human hepatic cell line utility as a surrogate for primary human hepatocytes in drug metabolism assessment in vitro. *J. Pharmacol. Toxicol. Methods* **63**, 59–68 (2011).
58. Sielaff, T. D. *et al.* Gel-entrapment bioartificial liver therapy in galactosamine hepatitis. *J. Surg. Res.* **59**, 179–184 (1995).
59. Newsome, P. N. *et al.* Development of an invasively monitored porcine model of acetaminophen-induced acute liver failure. *BMC Gastroenterol.* **10**, 34 (2010).
60. Kessler, M. A., Meinitzer, A. & Wolfbeis, O. S. Albumin blue 580 fluorescence assay for albumin. *Anal. Biochem.* **248**, 180–182 (1997).

## Author contributions

L.J.N. and J.N.P. conceived and designed the study; L.J.N. carried out experiments and had the primary role in writing the paper. L.J.N. and A.F.H. carried out assay development experiments. S.W.W., J.N.P. and P.C.H. contributed to data analysis and data interpretation. L.J.N. and P.T. carried out final data analysis and preparation. S.W.W., J.N.P., and P.C.H. supervised and advised on scientific aspects. All authors discussed results and provided comments for each draft of the manuscript.





## Additional information

Supplementary information accompanies this paper at <http://www.nature.com/scientificreports>

**Competing financial interests:** The authors declare no competing financial interests.

**How to cite this article:** Nelson, L.J. *et al.* Profiling the Impact of Medium Formulation on

Morphology and Functionality of Primary Hepatocytes *in vitro*. *Sci. Rep.* **3**, 2735; DOI:10.1038/srep02735 (2013).



This work is licensed under a Creative Commons Attribution-NonCommercial-ShareAlike 3.0 Unported license. To view a copy of this license, visit <http://creativecommons.org/licenses/by-nc-sa/3.0>